

A Continuous Contact Force Model for Highly Damped Impacts of Arbitrary Material and Geometry

Dylan A. Ramaswamy¹, J. Sean Humbert²

¹ Department of Mechanical Engineering
University of Colorado Boulder
Boulder, CO, 80309, United States
dylan.ramaswamy@colorado.edu

² Department of Mechanical Engineering
University of Colorado Boulder
Boulder, CO, 80309, United States
sean.humbert@colorado.edu

ABSTRACT

In this work, further analysis is done on the Hunt-Crossley contact force model to both better understand its behavior and estimate parameters. Through nondimensionalization, the model's damping and stiffness characteristics are presented in new ways, in terms of a damping ratio and natural frequency. These parameters lead to the derivation of a new form of the Hunt-Crossley model for use in practice. Additionally, the approximation for the velocity-deformation relationship throughout impact is improved so that its curvature may vary with increased damping. This improvement leads to the derivation of a new expression for the hysteresis damping coefficient that is accurate for highly damped impacts. To finish, work is done to allow for empirical determination of stiffness. Utilizing the derived natural frequency, an expression is generated so that the model stiffness can be determined from the total time of impact.

Keywords: Contact, Impact, Nonlinear Dynamics, Mechanics, Multibody.

1 INTRODUCTION

In 1975, Hunt and Crossley proposed the first mathematically valid model of dissipative impact. The Hunt-Crossley model prescribes the normal force throughout contact as

$$F_N = \lambda \delta^n \dot{\delta} + K \delta^n, \quad (1)$$

where λ is the hysteresis damping coefficient, K is the system stiffness, n is the Hertzian (or topological) exponent, and δ and $\dot{\delta}$ are the deformation and deformation rate (velocity) respectively [1]. The second term, $K \delta^n$, is the longstanding Hertz term which characterizes the stiffness effects of impact, while the first, $\lambda \delta^n \dot{\delta}$, was the Hunt-Crossley addition made to accommodate impact dissipation [2, 1]. This term is crucial, for all real-world impacts are dissipative, intrinsically hysteretic, and oftentimes to nonnegligible degrees.

The issue with the Hunt-Crossley model is that it is difficult to use in practice. Mathematically valid though it may be, the very inclusion of the damping term makes its use in applied simulation challenging. To model any real-world impact, each system parameter must be known: these are λ , K , and n . For the contact between linear elastic spheres, K is known, can be analytically formulated from conventional material descriptions; n is also known, derived from the geometry of the spheres [3]. λ , however, is more abstruse, amorphous, and at the time of Hunt-Crossley's formulation, had no analytical means of determination, as is still the case.

Hunt and Crossley addressed the issue via empirical relation. They proposed that if one could determine the coefficient of restitution of impact, an empirical parameter, it would be consequently possible to determine from it the model parameter, λ [1]. This is where the bulk of the work in the field has been done since 1975, in improving the relationship between λ and the coefficient of restitution, c_r [4, 5, 1, 3, 6].

The accuracy of this relationship is important, and further efforts will be made here to remedy certain inaccuracies that still exist in its prominent solutions. A principal point of this work, though,

is to emphasize the following about λ : it is but one piece of the puzzle. What about the other principal system parameter, the stiffness, K ? The tunneled focus on λ has left K mostly ignored in the field. Certain analytical expressions for K exist, yes, but *only* for simple cases, for impacts between linear elastic materials of simple geometry [3]. This limitation must be stressed. What about impacts between objects of nonstandard geometry, what about impacts between nonlinear elastic materials? For impacts of more general nature, there are currently no means available for determining the stiffness parameter. Even if λ can be determined, K cannot. This is to say that the Hunt-Crossley model is still unusable for most impacts in practice.

This paper is organized as follows: The subsequent section, Section 2, will begin with the reformulation of the Hunt-Crossley model. This reformulation will be useful in that new behavioral parameters of the model will be derived, allowing for the stiffness and damping characteristics to be expressed in more convenient forms. Section 3 will address the $\lambda(c_r)$ relationship and the areas where it still lacks accuracy. Correcting inaccuracies in the velocity-deformation relationship throughout impact, a new expression for $\lambda(c_r)$ will be produced that is accurate in the limit as $c_r \rightarrow 0$. The final section, section 4, will address the issue of stiffness. New theory will be developed so that K may be empirically determined, allowing for a first time method of stiffness determination in general cases, in impacts of both arbitrary material and geometry.

2 Reformulation of Hunt-Crossley

To derive a secondary form of the Hunt-Crossley model, it is necessary to nondimensionalize it. Nondimensionalization is a powerful tool in that it is modular, can be applied to linear or nonlinear systems, and allows one to study a differential equation in a purely behavioral sense. In differential form, the Hunt-Crossley model is written as [1]

$$m\ddot{\delta} + \lambda \delta^n \dot{\delta} + K\delta^n = 0. \quad (2)$$

This is the standard form of the dynamic equation. To translate it into dimensionless space, it is first necessary to define base dimensionless parameters for the system's dependent and independent variables. The base dimensionless parameters for the Hunt-Crossley model are selected to be

$$\begin{aligned} \dot{X} &= \frac{\dot{\delta}}{\dot{\delta}_0}, \\ \tau &= \omega_i t. \end{aligned} \quad (3)$$

Here, \dot{X} is the dimensionless velocity and τ the dimensionless time. \dot{X} is a function of τ , the same way $\dot{\delta}$ is a function of t in dimensional space. $\dot{\delta}_0$ is the incidence velocity, the velocity immediately before impact, and ω_i is some arbitrary time constant. That \dot{X} is selected as the base dependent variable is an important point of note. Oftentimes the zeroth derivative, X , is selected (as in the nondimensionalization of the Kelvin-Voigt model), but for Hunt-Crossley it is crucial to use \dot{X} . Velocity is what triggers impact, not deformation. Deformation is a response to the input, and as such has mathematically unbounded limits. The limits of velocity, conversely, *are* bounded; the velocity can only ever exist between $\pm\dot{\delta}_0$. Furthermore, $\dot{\delta}_0$ is a known parameter, making its use in the nondimensionalization process a necessity.

The expression for \dot{X} in (3) can be both integrated and differentiated to generate expressions for both X and \ddot{X} , the zeroth and second derivatives respectively. With these two relationships derived, all three of the dependent variable relationships can be presented in terms of dimensional as functions of dimensionless.

$$\begin{aligned} \delta &= \frac{\dot{\delta}_0}{\omega_i} X, \\ \dot{\delta} &= \dot{\delta}_0 \dot{X}, \\ \ddot{\delta} &= \omega_i \dot{\delta}_0 \ddot{X}. \end{aligned} \quad (4)$$

Substituting these relationships into equation (2), the Hunt-Crossley model can be brought into dimensionless space. With simplifications, the dimensionless equation follows:

$$\ddot{X} + \frac{\lambda \dot{\delta}_0^n}{m \omega_i^{n+1}} X^n \dot{X} + \frac{K \dot{\delta}_0^{n-1}}{m \omega_i^{n+1}} X^n = 0. \quad (5)$$

Note that the time constant, ω_i , factors into both the damping and stiffness terms. It can be derived here through normalization. Per standard procedure prescribed for second order differential equations, ω_i is derived through the normalization of the the stiffness term, X^n , rather than the damping term, $X^n \dot{X}$. Proceeding with this normalization and solving, ω_i results as follows:

$$\omega_i = \left[\frac{K \dot{\delta}_0^{n-1}}{m} \right]^{\frac{1}{n+1}}. \quad (6)$$

This is the undamped natural frequency of the Hunt-Crossley model. To differentiate it from the natural frequency of the Kelvin-Voigt model ($\omega_n = \sqrt{k/m}$), ω_i will be christened here as the *impact natural frequency*. Comparing it to ω_n , it can be noted that ω_i depends on the initial condition, $\dot{\delta}_0$, as well as both the stiffness and mass. Interestingly, when $n = 1$, when the impact is linearly stiff, velocity does not play a factor. Furthermore, when $n = 1$, ω_i is exactly equal to ω_n .

The expression for ω_i can be substituted into (5) to eliminate it from the equation. The result, after simplification, follows:

$$\ddot{X} + \frac{\lambda \dot{\delta}_0}{K} X^n \dot{X} + X^n = 0. \quad (7)$$

The only term remaining with values attached is the damping term. This allows one to determine that it is these parameters, and these parameters alone, that affect the damping characteristics of Hunt-Crossley impact. To simplify the equation fully, these three parameters will be grouped:

$$\varepsilon = \frac{\lambda \dot{\delta}_0}{K}. \quad (8)$$

ε is christened as the *hysteresis damping ratio*. Like with ω_i , the incidence velocity factors into its definition. An interesting insight from ε is that it is mass independent. Note that damping in Kelvin-Voigt, its damping ratio given by $\zeta = \frac{c}{2\sqrt{km}}$, does depend on the mass of the system. That damping in Hunt-Crossley is independent of mass is an interesting insight, and would be important to verify in experiment.

Substituting the definition of ε into the result in (7), the dimensionless equation simplifies to

$$\ddot{X} + \varepsilon X^n \dot{X} + X^n = 0. \quad (9)$$

This is the final form of the dimensionless Hunt-Crossley equation. Note that its boundary conditions are $X(0) = 0$ and $\dot{X}(0) = 1$. This form allows for pure behavioral study of the model's character. That only ε and n factor into its definition signifies that it is just these parameters that control the behavior of its solutions.

The final step is to generate a new dimensional form of Hunt-Crossley that incorporates the behavioral parameters ε and ω_i . This can be done by redimensionalizing equation (9). Using the relationships in (4) for the redimensionalization, the following equation is produced:

$$\ddot{\delta} + \frac{\omega_i^{n+1}}{\dot{\delta}_0^n} \delta^n (\varepsilon \dot{\delta} + \dot{\delta}_0) = 0. \quad (10)$$

This is a secondary form of the Hunt-Crossley model, its acceleration form. Its input parameters are ε , ω_i , and n . Note that the incidence velocity, $\dot{\delta}_0$, also factors as a parameter in its formulation. This form allows for one to characterize Hunt-Crossley's damping and stiffness properties in terms of the new parameters ε and ω_i rather than the traditional λ and K . This fact will be particularly important for the work done on stiffness characterization in section 4.

3 Damping as it relates to coefficient of restitution

Before tackling stiffness, the $\lambda(c_r)$ relationship is sought to be improved so that it is accurate in the limit as $c_r \rightarrow 0$. The relationship has existed in many forms, but the general form that will be built upon here is that of the Flores et al. and Hu-Guo solutions [4, 5].

The longstanding method for determining an expression for $\lambda(c_r)$, put forth initially by Hunt and Crossley themselves, is to solve for λ in the following dissipative energy balance [1]:

$$\oint \lambda \delta^n \dot{\delta} d\delta = \frac{1}{2} m \dot{\delta}_0^2 (1 - c_r^2). \quad (11)$$

The expression itself is an exact analytical one; both sides are merely different measures of the total energy lost in impact. The relation cannot be directly solved, however. It is for this reason that only approximate relationships for $\lambda(c_r)$ can be produced.

3.1 The velocity-deformation relationship

The issue in solving equation (11) stems from the $\dot{\delta}$ term in the cyclic integral. $\dot{\delta}$ is the relationship between velocity and deformation throughout impact (it will be denoted in this paper as $\dot{\delta}(\delta)$ to distinguish its dependence here on deformation separate to its dependence on time in the differential equation). As the Hunt-Crossley model is, in its general form, analytically unsolvable, it follows that no general analytical solution for $\dot{\delta}(\delta)$ can be determined. To solve equation (11), therefore, it is such that some approximate expression must be used.

The best approximation used currently for $\dot{\delta}(\delta)$, used by Flores et al., Hu-Guo, and others, is written below [4, 5, 6]:

$$\dot{\delta}(\delta) = \begin{cases} \dot{\delta}_c = \dot{\delta}_0 \left[1 - \left(\frac{\delta}{\delta_m} \right)^{n+1} \right]^{\frac{1}{2}}, \\ \dot{\delta}_r = -c_r \dot{\delta}_0 \left[1 - \left(\frac{\delta}{\delta_m} \right)^{n+1} \right]^{\frac{1}{2}}, \end{cases} \quad (12)$$

where δ_m is the maximum deformation. $\dot{\delta}(\delta)$ is a piecewise function, where $\dot{\delta}_c$ governs the relationship in the compression phase, and $\dot{\delta}_r$ governs it in restitution. This approximation is accurate in that it covers the bounds of the numerical $\dot{\delta}(\delta)$ solution, that which is the target of the approximation, perfectly. Where the description fails, however, is in mapping the curvature the numerical solution takes as damping increases.

Figure 1(a) displays both equation (12) and the numerical solution for a largely damped impact ($\varepsilon = 5$, $c_r \approx 0.2$). The failure in curvature mapping can be seen clearly. The specific failure is that the compression function overestimates the curve, whereas the restitution function underestimates it. The general trend for the numerical solution is that, with increased damping, the curvature of the compression profile becomes shallower while the curvature in restitution becomes sharper. Understanding this behavior, suitable changes to the velocity-deformation approximations can be made to better improve their accuracy. The approximations in this work are as follow:

$$\begin{aligned} \dot{\delta}_c &= \dot{\delta}_0 \left[1 - \left(\frac{\delta}{\delta_m} \right)^{n+1} \right]^{\frac{1}{2}+p}, \\ \dot{\delta}_r &= -c_r \dot{\delta}_0 \left[1 - \left(\frac{\delta}{\delta_m} \right)^{n+1} \right]^{\frac{1}{2}-p}. \end{aligned} \quad (13)$$

The only difference between these relationships and the previous is the addition of the variable p into the outer exponents. p is denoted as the curvature accommodation exponent. It was noted that the square root, the $1/2$ in equation (12), is what controls the curvature of the profiles. Allowing

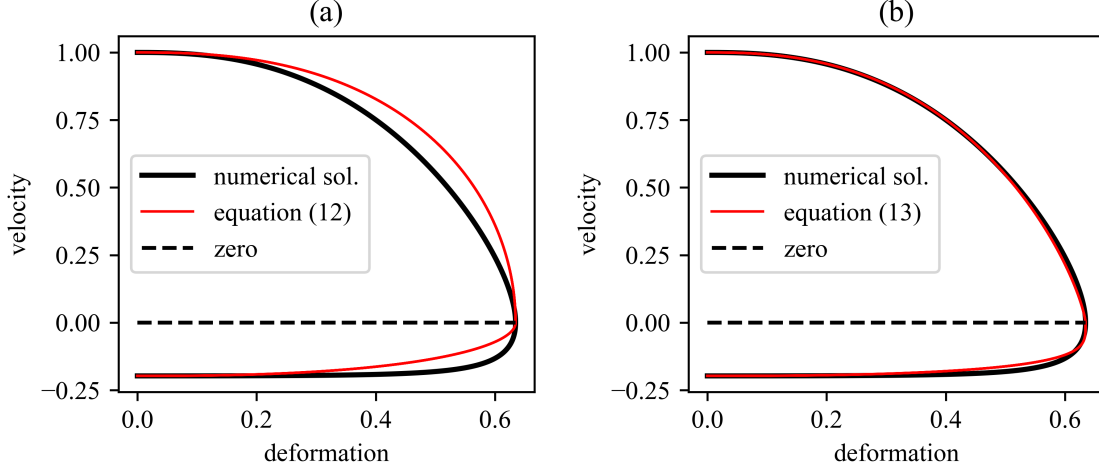


Figure 1. $\dot{\delta}(\delta)$ for $\varepsilon = 5$ ($c_r \approx 0.2$): (a) numerical solution and current best approximation, equation (12); (b) numerical solution and improved approximation, equation (13)

the exponents to vary by some factor, therefore, allows the curvature of the profiles to be adjusted. That the p is added in the compression function while it is subtracted in the restitution function is indicative of how the compression curve grows shallower while the restitution curve grows sharper with increased damping. It was observed that these respective growths follow similar rates, hence the use of the same p in both functions.

These approximations can be fit to the numerical solution to test their validity. As p factors into both functions, its value will be determined by the p that best fits *both* portions of the numerical solution, the compression and restitution curves simultaneously. Figure 1(b) presents the comparison of equation (13) to the numerical solution with best fit p . It is clear that this approximation represents the numerical solution much better than the previous incarnation. Albeit minor discrepancies still exist, the curvatures of both align almost perfectly. It is posited, therefore, that the improved accuracy in $\dot{\delta}(\delta)$ here will lead consequently to improved accuracy in the resulting $\lambda(c_r)$ expression, allowing for more precise determination of λ in the highly damped region.

The $\dot{\delta}(\delta)$ approximation must be analytically complete, however, before it can be used in the cyclic integral for solution. The completion lies in determining an expression for p . Note that the value of p will need to change depending on what level of damping exists. This is to say that the p in equation (13) is not a fixed value but rather a function that varies with damping: $p(c_r)$.

Plotting the numerical solution for how p changes with c_r , its general profile can be determined. $p(c_r)$, it was seen, follows decaying exponential trajectory. The function was furthermore determined to have bounded limits: at $c_r = 1$, $p = 0$, and as $c_r \rightarrow 0$, $p \rightarrow 1/2$. An expression that represents these behaviors follows:

$$p(c_r) = \alpha(e^{-\beta c_r} - e^{-\beta}). \quad (14)$$

Here, α and β are numerical constants. Note that the use of function is not restricted to that selected here. There are many suitable choices. A decaying logarithm could have been used instead, for example. The only restriction is that the function exhibits decaying behavior with increasing coefficient of restitution.

3.2 Hysteresis damping coefficient/ratio

With a complete form of the $\dot{\delta}(\delta)$ approximation, the integral in equation (11) can be computed. Substituting (13) into (11) and solving, the hysteresis damping coefficient, with p kept as a vari-

able, results as follows:

$$\lambda(c_r) = \frac{K(3+2p)(1-c_r^2)}{2c_r\delta_0} \left(\frac{3+2p}{3-2p} + c_r \right)^{-1}. \quad (15)$$

Note that when p is set equal to zero, this solution is exactly equal to that proposed by Hu-Guo [5]. Using the definition of the hysteresis damping ratio in equation (8), the result can be presented in terms of ε :

$$\varepsilon(c_r) = \frac{(3+2p)(1-c_r^2)}{2c_r} \left(\frac{3+2p}{3-2p} + c_r \right)^{-1}. \quad (16)$$

The final step to complete the approximation is to substitute in the expression for p , equation (14), and determine the constants α and β . The complete expression for $\varepsilon(c_r)$ follows below:

$$\varepsilon(c_r) = \frac{(3+2\alpha(e^{-\beta c_r} - e^{-\beta}))(1-c_r^2)}{2c_r} \left(\frac{3+2\alpha(e^{-\beta c_r} - e^{-\beta})}{3-2\alpha(e^{-\beta c_r} - e^{-\beta})} + c_r \right)^{-1}. \quad (17)$$

To compute the constants, equation (17) can be applied to the numerical $\varepsilon(c_r)$ solution to produce a best fit. Figure 2 displays the best fit of equation (17) to the numerical solution. The constants produced by the fit are $\alpha = 1.381$ and $\beta = 0.451$.

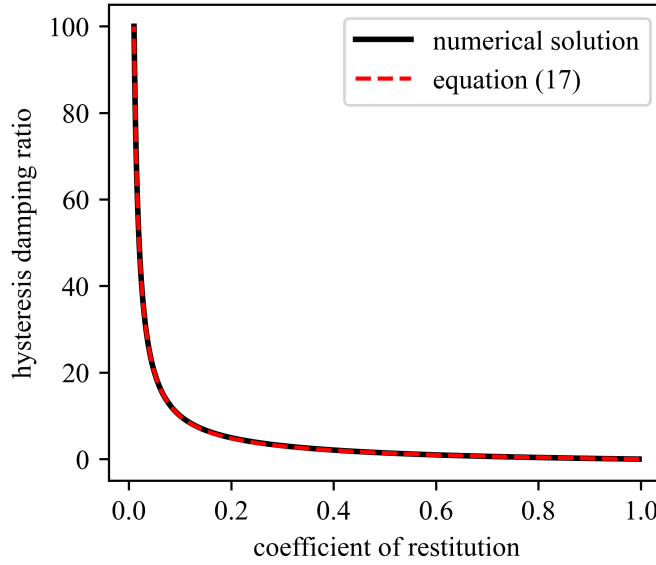


Figure 2. Numerical and approximate solution to $\varepsilon(c_r)$ for $0.01 \leq c_r \leq 1.0$

It can be seen that the approximation does exceptionally well at mapping the numerical solution, in both curvature and magnitude. The computed relative error between the two curves, over the range $0.01 \leq c_r \leq 1.0$ (or $0 \leq \varepsilon \leq 100$), is 0.062%. This fractional error confirms equation (17)'s validity for use in the limit as $c_r \rightarrow 0$, as with all ranges of damping.

That equation (17) is presented in terms of ε instead of λ is a conscious choice. In this analysis, ε is far more useful. All simulations in this section were done with the dimensionless model, equation (9), as will be the case for section 4. It will be seen that working in terms of ε is not just a matter of convenience, but an actual requirement for the theory developments that follow.

4 Stiffness as it relates to impact time

To allow for the highest practicality of the Hunt-Crossley model, it needs to be possible to determine generally not just the model's damping characteristics, as has been done, but its stiffness characteristics as well. As is the case with λ , the best way to do this is through empirical relation.

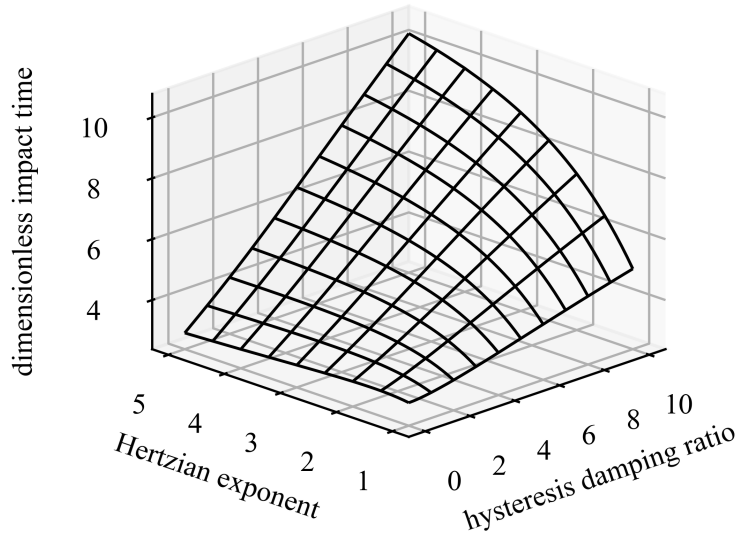


Figure 3. Numerical solution to $\Delta\tau(\varepsilon, n)$ for $0 \leq \varepsilon \leq 10$ and $1 \leq n \leq 5$

To create an empirical relationship for stiffness, it is first necessary to relate K to some measurable experimental parameter, the same way λ is related to c_r . To determine what the empirical parameter should be, it is easier to think about the stiffness in terms of the impact natural frequency, ω_i , rather than K . The reason for this is because, while it is not readily apparent what empirical parameter could directly relate to K , with natural frequency, its very units signify its relation to time. The empirical parameter selected, therefore, is time. Specifically, it is the total time of impact, Δt .

To generate an expression for ω_i in terms of Δt , it will be easier to use the dimensionless form of Hunt-Crossley, equation (9), and translate into dimensional space at the end. This translation can be done with the dimensional-dimensionless time relationship shown in equation (3). Writing the relationship in a different form, the impact natural frequency can be expressed as

$$\omega_i = \frac{\Delta\tau}{\Delta t}. \quad (18)$$

This is to say that the natural frequency can be computed if one knows both the dimensional and dimensionless impact times. The principal aim of this analysis, then, is to determine some variable expression for $\Delta\tau$.

4.1 Dimensionless impact time

Characterization of $\Delta\tau$ will be done through simulation of the dimensionless equation. Noting that both ε and n control the behavior of its solutions, it can be posited that $\Delta\tau$ will be a multi-variable function: $\Delta\tau(\varepsilon, n)$. This makes the process of representing it functionally a matter more complicated than with single-variable phenomena.

The first step is to simulate its behavior. Figure 3 presents the numerical solution for $\Delta\tau(\varepsilon, n)$. This is the target surface that is sought to be functionally expressed. To generate such an expression, it is most tractable to approach the solution in parts. First, it will be studied how $\Delta\tau(\varepsilon, n)$ behaves when $n = 1$. This simplifies the problem by a reduction to one dimension. Determining a single-variable expression to approximate $\Delta\tau(\varepsilon, 1)$, this base expression can then be adjusted to accommodate how it behaves with varying n , i.e., made multivariable. This will produce $\Delta\tau(\varepsilon, n)$.

Beginning with $n = 1$, it can be noticed from Figure 3 that $\Delta\tau(\varepsilon, 1)$ begins with exponential growth but assumes pure linear behavior past $\varepsilon = 3$. The base function, therefore, can take the form of a

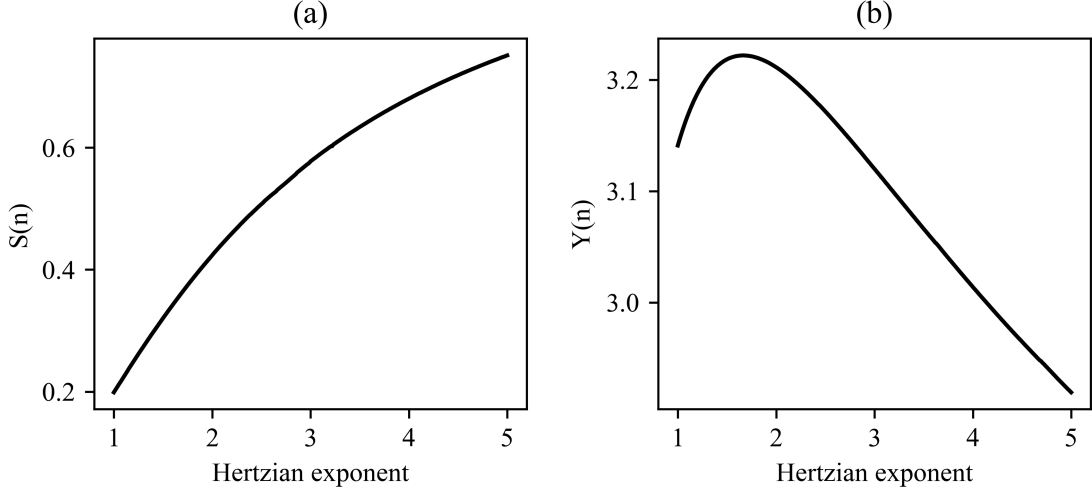


Figure 4. (a) Numerical $S(n)$ solution, (b) numerical $Y(n)$ solution (undamped $\Delta\tau$)

coupled linear-exponential relationship. The general form of such a relationship follows as

$$\Delta\tau(\varepsilon, 1) = ae^{-b\varepsilon} + c\varepsilon + d, \quad (19)$$

where a , b , c , and d are numerical constants.

From here, it is necessary to understand what aspects of $\Delta\tau(\varepsilon, 1)$'s behavior changes when n is allowed to vary. Two key changes can be noted from Figure 3. The first is the intercept, or the undamped impact time, and the second is the curves' slopes. Both of these aspects of the $\Delta\tau(\varepsilon, 1)$ curve change with increasing n . Incorporating these two factors into equation (19), a general form for $\Delta\tau(\varepsilon, n)$ is formulated:

$$\Delta\tau(\varepsilon, n) = ae^{-b\varepsilon} + S(n)\varepsilon + Y(n). \quad (20)$$

Here, $S(n)$ is denoted as the slope function, and $Y(n)$ is denoted as the intercept function. $S(n)$ replaces the constant c while $Y(n)$ replaces the constant d . These adjustments allow for the expression to accommodate the discussed behavioral changes with increasing n .

It is from here necessary to determine suitable functions for both $S(n)$ and $Y(n)$ so that equation (20) is analytically complete. To do so, the numerical solution for both functions can be plotted and expressions can be made to approximate them. Figure 4 displays the numerical solutions.

Looking first at the numerical slope function, $S(n)$, in Figure 4(a), its profile appears to be governed by decaying exponential behavior, albeit inverted. This behavior can be encompassed analytically by the following general expression:

$$S(n) = c - de^{-fn}. \quad (21)$$

Regarding the numerical intercept function, $Y(n)$, shown in Figure 4(b), it can be seen that its behavior is more nuanced. Encapsulating its behavior will require a combination of elementary functions. Its behavior can be broken into two parts, that before $n = 3$ and that after. Before $n = 3$, the profile behaves similarly to xe^{-x} , while after $n = 3$, it behaves linearly, $-x$. Combining the two, the form of the approximation is $xe^{-x} - x$. Written generally, the approximate intercept function follows below. The numerical constants here are g , h , i , j , and k . Note that all five are necessary for accurate fitting.

$$Y(n) = (gn - h)e^{-in} - jn + k. \quad (22)$$

With suitable approximations determined for $S(n)$ and $Y(n)$, they can be substituted into equation (20). The expression with these substitutions follows as

$$\Delta\tau(\varepsilon, n) = ae^{-b\varepsilon} + (c - de^{-fn})\varepsilon + (gn - h)e^{-in} - jn + k. \quad (23)$$

Note that there are a total of ten numerical constants in this expression, while e is retained as Euler's Number. Like with $\varepsilon(c_r)$ in section 3, the expression in (23) can be fit to the numerical solution to produce best-fitted constants.

Figure 5 shows the fit of equation (23) to the numerical solution. The constants produced are $a = 0.180$, $b = 0.880$, $c = 0.853$, $d = 1.018$, $f = 0.461$, $g = 1.434$, $h = 0.864$, $i = 0.771$, $j = 0.023$, and $k = 2.695$. The computed relative error between the two surfaces is 0.237%.

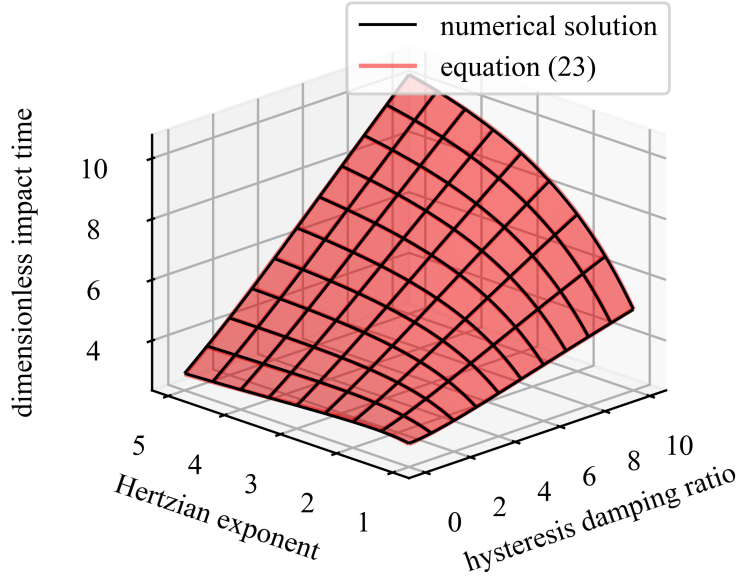


Figure 5. Numerical and approximate solution to $\Delta\tau(\varepsilon, n)$ for $0 \leq \varepsilon \leq 10$ and $1 \leq n \leq 5$

4.2 Natural frequency and stiffness

It is from here that the natural frequency can be derived. The expression for dimensionless impact time in (23), having been confirmed accurate, can be translated into dimensional space through equation (18). This substitution results in the sought after expression for natural frequency as a function of dimensional impact time:

$$\omega_i(\varepsilon, n, \Delta t) = \frac{1}{\Delta t} \left[ae^{-b\varepsilon} + (c - de^{-fn})\varepsilon + (gn - h)e^{-in} - jn + k \right]. \quad (24)$$

This ω_i can be used in equation (10), in the acceleration form of Hunt-Crossley, for simulation. If the standard form is desired to be used, however, one will need an expression explicitly for K . This can be derived through equating the above expression for ω_i with its analytical definition in equation (6). Solving for K , the following is produced:

$$K = \frac{m}{\delta_0^{n-1}} \left(\frac{1}{\Delta t} \left[ae^{-b\varepsilon} + (c - de^{-fn})\varepsilon + (gn - h)e^{-in} - jn + k \right] \right)^{n+1}. \quad (25)$$

These are the final forms. Either expression will allow for the Hunt-Crossley model's stiffness input to be determined purely from experiment. This method is powerful in that it is modular, can be used for impacts between objects of arbitrary nature. So long as one can measure accurately

both the coefficient of restitution and total time of impact, as well as the Hertzian exponent, materials of either linear or nonlinear character can be represented by the model. This removes the requirement of an analytical expression for stiffness determination.

5 CONCLUSIONS

The aim of this work was to provide improved theory for the Hunt-Crossley contact force model so that its use may be more widespread. For use in general applications, modular methods need to be in place to determine accurately the model's damping and stiffness parameters. Through translation into dimensionless space, it was shown possible to characterize the model's damping and stiffness in terms of new parameters. The hysteresis damping ratio, ε , allows damping to be characterized nondimensionally, while the impact natural frequency, ω_i , allows stiffness to be characterized with relation to time. These two parameters led to the derivation of a new form of the Hunt-Crossley model, in units of acceleration rather than force, that incorporates ε and ω_i as inputs instead of λ and K .

Work followed to allow for accurate determination of the discussed model parameters. Building off the work of the literature, a new relationship between λ/ε and the coefficient of restitution was produced. Through additions to the velocity-deformation relationship, allowing for changes in curvature, it was shown that a new $\lambda/\varepsilon(c_r)$ expression could be produced for high accuracy in all ranges of coefficient of restitution, specifically as $c_r \rightarrow 0$.

For stiffness, entirely new methods were put forth to determine its value empirically. Recognizing stiffness to be related to the total time of impact, Δt , it was possible to generate a relationship between Δt and the impact natural frequency. Dimensionless study allowed for further insight, that ω_i is not purely a function of Δt but of ε and n as well: $\omega_i(\varepsilon, n, \Delta t)$. This expression allows for first time determination of stiffness for general case impacts. Characterizing the stiffness in this way, the Hunt-Crossley model can be used to simulate a much wider range of impact scenarios in practice.

REFERENCES

- [1] Hunt, K.H., Crossley, F.R.E.: Coefficient of restitution interpreted as damping in vibroimpact. (1975)
- [2] Hertz, H.: The contact of elastic solids. *J Reine Angew, Math* **92** (1881) 156–171
- [3] Lankarani, H.M., Nikravesh, P.: A contact force model with hysteresis damping for impact analysis of multibody systems. In: *International Design Engineering Technical Conferences and Computers and Information in Engineering Conference*. Volume 3691., American Society of Mechanical Engineers (1989) 45–51
- [4] Flores, P., Machado, M., Silva, M.T., Martins, J.M.: On the continuous contact force models for soft materials in multibody dynamics. *Multibody system dynamics* **25** (2011) 357–375
- [5] Hu, S., Guo, X.: A dissipative contact force model for impact analysis in multibody dynamics. *Multibody System Dynamics* **35** (2015) 131–151
- [6] Zhang, J., Li, W., Zhao, L., He, G.: A continuous contact force model for impact analysis in multibody dynamics. *Mechanism and Machine Theory* **153** (2020) 103946